SPECTRAL CORRELATION AND JEFFRIES-MATUSITA BASED MATCHING ALGORITHM FOR IMPROVED INFORMATION EXTRACTION FROM HYPERSPECTRAL IMAGES

Padma S[1] and Sanjeevi S[2]

[1] Department of Civil Engineering, Saveetha Engineering College, Saveetha Nagar, Thandalam, Chennai, India.
Email: padmagi91@gmail.com

[2] Department of Geology, Anna University, Sardar Patel Road, Guindy, Chennai, India.
Email: ssanjeevi@annauniv.edu

KEY WORDS: Hyperspectral remote sensing, Spectral Correlation Mapper, Jeffries-Matusita, Spectral Matching Index

ABSTRACT: Enhanced information extraction from hyperspectral imagery is usually achieved by applying the individual spectral matching approaches like Spectral Angle Mapper (SAM), Spectral Correlation Mapper (SCM) and Jeffries-Matusita distance (JM) independently. However, there is a tendency to overestimate the strength of match by SCM, leading to false predictions. A hybrid algorithm is presented by combining stochastic measure (Jeffries-Matusita distance) and Spectral Correlation Mapper, which suppresses such an overestimation. The proposed algorithm is used to map the mangroves ecosystem in the Pichavaram and Muthupet ecosystems of southern India, where the complexity of the ecosystems poses a challenge to species level mapping.

The algorithm is used to match the unknown target (in EO-1 Hyperion image) with the reference spectra of the spectral library, compiled from the image. Reference spectra for Pichavaram are of *Avicennia*, *Rhizopora*, paddy, groundnut, mudflat, sand, clear water and shallow water. For Muthupet, they are for *Avicennia*, *Prosopis*, plantation, marsh, mudflat, sand, clear water and shallow water. The matching algorithm and supervised approach are used to classify the image. The performance of JM-SCM is compared with JM-SAM, JM, SCM and SAM using the Relative Spectral Discriminatory Probability (RSDPB) and Relative Spectral Discriminatory Entropy (RSDE) measures. It is inferred that the JM-SCM algorithm results in higher accuracy compared to its individual components. False alarms were seen for SCM since it overestimated the area of groundnut in Pichavaram and *Prosopis* in Muthupet. The JM-SCM suppressed these alarms, leading to improved results. Compared to JM-SAM, JM-SCM discriminated clear and shallow waters better. SMI (Spectral Matching Index), a parameter that indicates the relationship between false alarms and detection rate, and hence the performance of JM-SCM measures, is introduced by the authors.

SCM identifies the linear relationship and detects the spectral shape between the two vectors, while JM computes the band-wise spectral information between the two vectors. The superiority of JM-SCM and accurate mapping of mangroves is attributed to the simultaneous utilization of spectral and spatial information.

1. INTRODUCTION

1.1 Spectral Matching Measures

The effectiveness of information extraction from remote sensing images is dependent on the quality of the data and the process involved in analyzing the data. The advent of various hyperspectral missions has facilitated the characterization of terrain and planetary surfaces in a precise manner. The contiguous bands of hyperspectral data with high spectral resolution accurately identifies materials based on their spectral features (Goetz et al., 1985). Compared to the spatial based classification techniques, spectral based approaches are effective in analyzing the hyperspectral data (Chang, 2003). The primary component in spectral based approaches is the spectral signature or spectrum which depicts the variations of reflectance of the surface materials, which is used in spectral matching. Unlike multispectral data, the spectrum generated from each pixel in a hyperspectral data characterizes the material based on its unique diagnostic features. Due to the relevance of such signatures and to facilitate spectral matching, several centralized spectral libraries or spectral databases with reference spectra of known materials are created. These libraries comprise of various spectra obtained from ground based spectral measurements and from hyperspectral images.

Spectral Matching involves the labeling of an unknown 'target' spectrum based on its closeness with the known 'reference' spectra. Based on the parameters considered for matching, these approaches are classified as (i) deterministic and (ii) stochastic. The deterministic algorithms Euclidean Distance Measure (ED), Spectral Angle Mapper (SAM), Spectral Correlation Measure (SCM), Binary Encoding (BE), and Spectral Feature Fitting (SFF) consider the geometrical and physical aspects of the target and reference spectra Stochastic algorithms Spectral Information Divergence (SID) and Constrained Energy Minimization (CEM consider the distributions of the spectral

reflectance of target (Vishnu et al., 2013; Shanmugam and SrinvasaPerumal, 2014). To overcome the limitations of individual approaches and to integrate their advantages, combined or hybrid approaches are developed. Such approaches outperform the individual components, *viz*. Spectral Information Divergence-Spectral Angle Mapper measure (SID-SAM) (Du et al., 2004), Spectral Information Divergence-Spectral Correlation Angle (SID-SCA) (Naresh Kumar et al., 2011) and Jeffries-Matusita distance as JM-SAM (Padma and Sanjeevi, 2014). In continuation of such developments, this study proposes a hybrid matching approach involving Jeffries-Matusita distance (JM) and Spectral Correlation Mapper (SCM) for efficient information extraction from hyperspectral images.

1.2 Spectral Angle Mapper (SAM)

Spectral Angle Mapper (SAM) is a deterministic approach which measures the spectral angle (θ) between the target spectrum (t) and the reference spectra (r) along a wavelength λ (Kruse et al., 1993). The smaller angle indicates higher spectral similarity. The spectral angle $\theta_{(t,r)}$ given by Equation (1) varies from 0 to 1.57 radians.

$$\theta_{(t,r)} = \cos^{-1}\left[\frac{\int t(\lambda)r(\lambda)d\lambda}{[\int t(\lambda)d\lambda]^{\frac{1}{2}}[\int r(\lambda)]}\right] \quad (1)$$

The advantages of the SAM approach are its tolerance to extent and illumination of the pixel. Being a computationally simple and fast measure, SAM is commonly used for varied applications. SAM is the basis of angle based spectral matching approaches which was later improvised in several forms as Modified Spectral Angle Mapper (MSAM) (Staenz et al., 1999), Spectral Correlation Angle (SCA) and Spectral Gradient Angle (SGA) (Robila and Gershman, 2005), Optimized Spectral Angle Mapper (OSAM) (Bertels et al., 2005) and Enhanced Spectral Angle Mapper (ESAM) (Li et al., 2014).

1.3 Jeffries-Matusita Distance (JM)

Jeffries Matusita distance (JM) is a stochastic approach which measures the separability of the target and reference spectral vectors. The probability density of the target and reference spectral vectors, t and r for bands (l=1,2…L) is p_l and q_l and the JM distance is :

$$\mathrm{JMD}(t,r) = \sqrt{\sum_{l=1}^{L}[\sqrt{p_l} - \sqrt{q_l}]^2} \quad (2)$$

For labeling a target spectrum, the concept of separability and matching are considered to be similar. The least distance measure between the classes assessed during separability is similar to the least probabilistic or geometrical measure between the reference and target spectra during spectral matching (Padma and Sanjeevi, 2014).

1.4 Combined Jeffries-Matusita-Spectral Angle Mapper Measures (JM-SAM)

The Jeffries-Matusita-Spectral Angle Mapper (JM-SAM) algorithm was developed by combining the deterministic Spectral Angle Mapper (SAM) and the stochastic Jeffries-Matusita Measure (JM) using the tangent and sine functions (Padma and Sanjeevi, 2014). The tangent and sine trigonometric functions are used to calculate the perpendicular distance between the target and reference (t and r) respectively as follows:

$$\text{JM-SAM(TAN)} = \text{JM(t, r) x tan(SAM(t, r))} \quad (3)$$
$$\text{JM-SAM(SIN)} = \text{JM(t, r) x sin(SAM(t, r))} \quad (4)$$

JM-SAM algorithm performs better than the individual JM and SAM approaches due to the simultaneous utilization of both geometrical and probabilistic aspects between the target and reference spectra. Further, the role of JM in using the band-wise spectral information yields improved results.

1.5 Improvised Spectral Angle Measure – Spectral Correlation Mapper (SCM)

One of the major limitations of SAM is its inability to distinguish between negative and positive correlations, since it considers only absolute values (De Carvalho and Meneses, 2000; Robila and Gershman, 2005 and Naresh Kumar et al., 2011). When a spectrum is modeled as a vector, there is a need to consider both the magnitude and direction parameters (Granahan, 2001; Homayouni and Roux, 2004). While direction corresponds to the shape which details each diagnostic feature present in the spectrum, magnitude corresponds to brightness of the pixel which yielded the spectrum. SAM utilizes only the direction to compute the spectral angle, and not the entire length of the spectral vector. Hence, SAM tends to be insensitive to unknown and variable illumination (Kruse et al., 1997). This may lead

to incorrect matching of a poorly illuminated target pixel. These limitations were overcome by one of the modified versions of Spectral Angle Mapper (SAM), namely Spectral Correlation Mapper (SCM) (De Carvalho and Meneses, 2000), which quantified the matching between the spectral vectors based on the parameter called 'correlation'. Correlation is a bivariate analysis that measures the strengths of association between two variables. This statistical parameter behaves in a physical space to capture the spectral shape between two vectors by following the entire length of the vector. One of its type's, namely Pearsonian correlation coefficient is sensitive to the linear relationship between two variables. SCM which is a derivative of Pearsonian correlation coefficient (R), normalizes and centres the coefficient measure on the average of the target (t) and reference spectra (r) as in Equation 5:

$$R = \frac{\Sigma(t-\bar{t})\Sigma(r-\bar{r})}{\sqrt{\Sigma(t-\bar{t})^2\Sigma(r-\bar{r})^2}} \quad (5)$$

$$\text{SCM} = cos^{-1}(R) \quad (6)$$

R varies from -1 to + 1, based on negative and positive correlation. However, to compare these values with SAM, the SCM measures are presented in radians (Equation 6) which varies from 0 to 1.57 radians.

2. DEVELOPMENT AND IMPLEMENTATION OF THE PROPOSED ALGORITHM

2.1 Jeffries-Matusita-Spectral Correlation Mapper Measure (JM-SCM)

The proposed Jeffries-Matusita - Spectral Correlation Mapper algorithm involves the incorporation of Spectral Correlation Mapper with Jeffries-Matusita Distance measure using tangent and sine measures as follows:

$$\text{JM-SCM(TAN)} = \text{JM(t, r) x tan(SCM(t, r))} \quad (7)$$
$$\text{JM-SCM(SIN)} = \text{JM(t,r) x sin(SCM(t,r))} \quad (8)$$

The tangent and sine trigonometric functions are used to calculate the perpendicular distance between the target and reference (t and r) respectively, instead of the cosine function which projects one spectrum along the other (Du et al., 2004 and Naresh Kumar et al., 2011).
Hence, both SCM and JM measures, though being stochastic in nature, behave deterministically as an angle and distance measure. Both these measures tend to utilize the entire length of the spectral vector in computing the correlation angle and self-information component. The best match in JM-SCM algorithm is characterized by the least-separable distance and least correlation angle between the spectral vectors at each band.
The implementation of the combined spectral matching algorithm was done in the MATLAB environment.

2.2 JM-SCM algorithm to map mangroves

The proposed JM-SCM matching algorithm is implemented to map the mangrove species and their associations in the Pichavaram and Muthupet mangrove ecosystems of southern India, where species level mapping is a challenge posed by the complexity of the ecosystem. The proposed algorithm is used to match the spectrum of an unknown target in the EO-1 Hyperion image, with the reference spectra of the spectral library, compiled from the known pixels in the image. The reference spectra for the Pichavaram region pertains to *Avicennia*, *Rhizopora*, paddy, groundnut, mudflat, sand, clear water and turbid water, while for Muthupet, it pertains to *Avicennia*, *Prosopis*, plantation, marsh, mudflat, sand, clear water and turbid water. Initially, a pixel level matching is carried out amongst the members of the compiled spectral library to assess the discriminability and matching ability of algorithm. This analysis was further extended into a supervised classification framework, where several target pixels from the image were matched with the reference spectra present in the library.

2.3 Performance Measures

The performances of the proposed JM-SCM algorithms are compared with JM-SAM, JM, SCM and SAM approaches based on: (i) relative spectral discriminatory probability (RSDPB), (ii) relative spectral discriminatory entropy (RSDE) and (iii) classification accuracy assessment.

2.3.1 Relative Spectral Discriminatory Probability (RSDPB): The relative spectral discriminatory probability (RSDPB) (Chang 2003; Du et al., 2004; Dudeni et al., 2009), is the measure of likelihood of identifying the target signature 't' from a set of spectral signatures or spectral library, Δ. For a spectral library Δ, comprising of 'K' signatures (r_1, r_2,…r_k), the RSDPB measure (Chang, 2003) is given as:

$$p^{m}_{t,\Delta}(k) = \frac{m(t,r_k)}{\sum_{j=1}^{L} m(t,r_j)} \quad (9)$$

where, $\sum_{j=1}^{L} m(t,S_j)$ is the normalization constant determined by the spectral matching measures in identifying target 't' from the set of reference spectra or spectral library 'Δ'. $m(t,r_k)$ is the spectral matching measure between the target spectra relative to the reference spectra S_k in the library Δ. From the resulting RSDPB vector, $[p^{m}_{t,\Delta}(r_1), p^{m}_{t,\Delta}(r_2),\ldots. p^{m}_{t,\Delta}(r_k)]^T$, the reference unit with a least relative probability is assumed as the best match for the target. The measure of likelihood of the matching algorithms in discriminating the spectral classes is presented as RSDPB plots. From these plots shown in Figure (2) and (5), it can be observed that the RSDPB value is lower while discriminating similar classes and higher while discriminating dissimilar classes.

2.3.2 Relative Spectral Discriminatory Entropy (RSDE): Using the RSDPB vector $[p^{m}_{t,\Delta}(r_1), p^{m}_{t,\Delta}(r_2),\ldots. p^{m}_{t,\Delta}(r_k)]^T$, the RSDE (Chang, 2003, Du et al., 2004 and Dudeni et al., 2009) measures the uncertainty in matching the target spectra (t) with the reference spectra in the spectral library (Δ). The RSDE measure is given as:

$$H^{m}_{RSDE}(t,\Delta) = -\sum_{k=1}^{K} p^{m}_{t,\Delta}(r_K)\log_2 p^{m}_{t,\Delta}(r_K) \quad (10)$$

It may be noted that, larger the value of $H^{m}_{RSDE}(t,\Delta)$, smaller is the chance of identifying a target 't' from a set of reference spectra in the library Δ. The measure of entropy of the matching algorithms in discriminating the spectral classes is presented as RSDE plots. From these plots shown in Figure (3) and (6), the range of uncertainty of the matching algorithms in assessing the correct match can be observed.

2.3.3. Accuracy Assessment: To estimate the percentage of correctly classified or matched pixels, post-classification accuracy assessment is carried out. Here, around 80 ground truth pixels identified from respective landcover samples are selected in the classified image through a stratified random process for accuracy estimation using the ERDAS Imagine package and validated using Google Earth (Geo-Eye-I) image.

2.4 Development of spectral matching index

False alarms or false hits represent the overestimation in the distribution of a target in the classification. The confusion matrix obtained from the accuracy assessment presented the correct and incorrect predictions made by the spectral matching algorithms (as classifiers). The sensitivity of the algorithm represents the proportion of the targets correctly predicted and is termed as 'true positive rate' or probability of detection (Pd). The specificity of the algorithm represents the proportion of the non-targets correctly predicted and is termed as 'true negative rate'. Both these parameters indicate the level of uncertainty in the classification. '100-specificity' quantifies the false positive rate which is known as probability of false alarm (Pf). High sensitivity is usually associated with poor specificity, which results in the overestimation of target pixels leading to false hits (Alatorre et al., 2011). The variation of sensitivity (Pd) and 100-specificity (Pf) for each matching algorithm are presented in Table (1) and (2).

To analyze the relationship between probability of detection and probability of false alarms with the spectral matching results; a new index called 'Spectral Matching Index' (SMI) is introduced (Equation 11).

$$SMI = \frac{Pf}{Pd} \quad (11)$$

This index computes the ratio of probability of false alarms to the probability of detection. SMI ranges from 0 to ∞. The goodness of the proposed matching algorithm is high near 0. SMI values for the matching algorithm in identifying the spectral classes are presented in Table (1) and (2) from which the matching algorithm with optimal range of SMI, required for low false alarm and higher detection, can be identified.

3. RESULTS AND DISCUSSION

3.1 Study Site I – Pichavaram Mangrove Ecosystem, Southern India

The results of the classification based on the spectral matching approaches for SCM, JM-SCM(TAN), JM-SCM(SIN), SAM, JM, JM-SAM(TAN) and JM-SAM(SIN) are shown in Figure (1). The spectral matching values amongst the reference classes (*Avicennia*, *Rhizopora*, paddy, groundnut, mudflat, sand, clear water and turbid water follows the order: JM-SCM(TAN)<JM-SCM(SIN)<JM-SCM(TAN)<JM-SCM(SIN)<JM<SCM<SAM. The least matching value indicates higher discrimination between the target and reference spectra.

The better performance of the JM-SCM algorithms can be observed from the RSDPB plots as shown in the Figure (2). While discriminating spectrally similar classes such as Avicennia and Rhizopora, the likelihood parameter for JM-SCM(TAN) and JM-SCM(SIN) is 0.0048 and 0.0104 compared to 0.0102, 0.0111, 0.038, 0.0463, 0.0493

respectively for JM-SAM(TAN), JM-SAM(SIN), SCM, SAM and JM. For dissimilar classes such as *Avicennia* and *Rhizopora*, the likelihood parameter for JM-SCM(TAN) and JM-SCM(SIN) is 0.8867 and 0.5637 compared to 0.6389, 0.6070, 0.4039, 0.3787 and 0.3716 respectively for JM-SAM(TAN), JM-SAM(SIN), SCM, SAM and JM. The least and highest value of JM-SCM measures in assessing the match between similar and dissimilar classes indicates its increased discriminability. This improved performance can be attributed to the nature of JM-SCM measure to compute the least spectral correlation angle and stochastic distance along the entire length of the spectrum. Such a discrimination is reflected in the quantum of accuracy of classification where the JM-SCM(TAN) and JM-SCM(SIN) have an higher accuracy of 93.75 % and 91.25 %. The accuracy of JM-SAM(TAN), JM-SAM(SIN), JM, SCM, SAM are 86.25%, 85 %, 76.25%, 75% and 71.25 % respectively. The higher accuracy of JM-SCM measures is due to the lesser uncertainty in identifying the correct matches shown as RSDE plots (Figure 3).
From Table 1, it can be observed that for paddy, SCM has a lower detection rate of 55.6% with a false alarm in the range of 50 %. From the accuracy assessment, it was observed that most of the target paddy was classified as groundnut leading to an overestimation of the latter, with a detection rate of 66.7%. This overestimation of groundnut was suppressed as JM-SCM(TAN) and JM-SCM(SIN) resulted in a higher detection rate of (90.9%) and (81.8%). This was reflected in Table 1, where the SMI of JM-SCM measures in identifying paddy was the least (0.13, 0.25) compared to 0.90 of SCM. The SMI for JM-SCM measures in identifying each class was the least compared to other matching measures, thereby indicating its goodness in resulting in higher detection with lower false alarm.

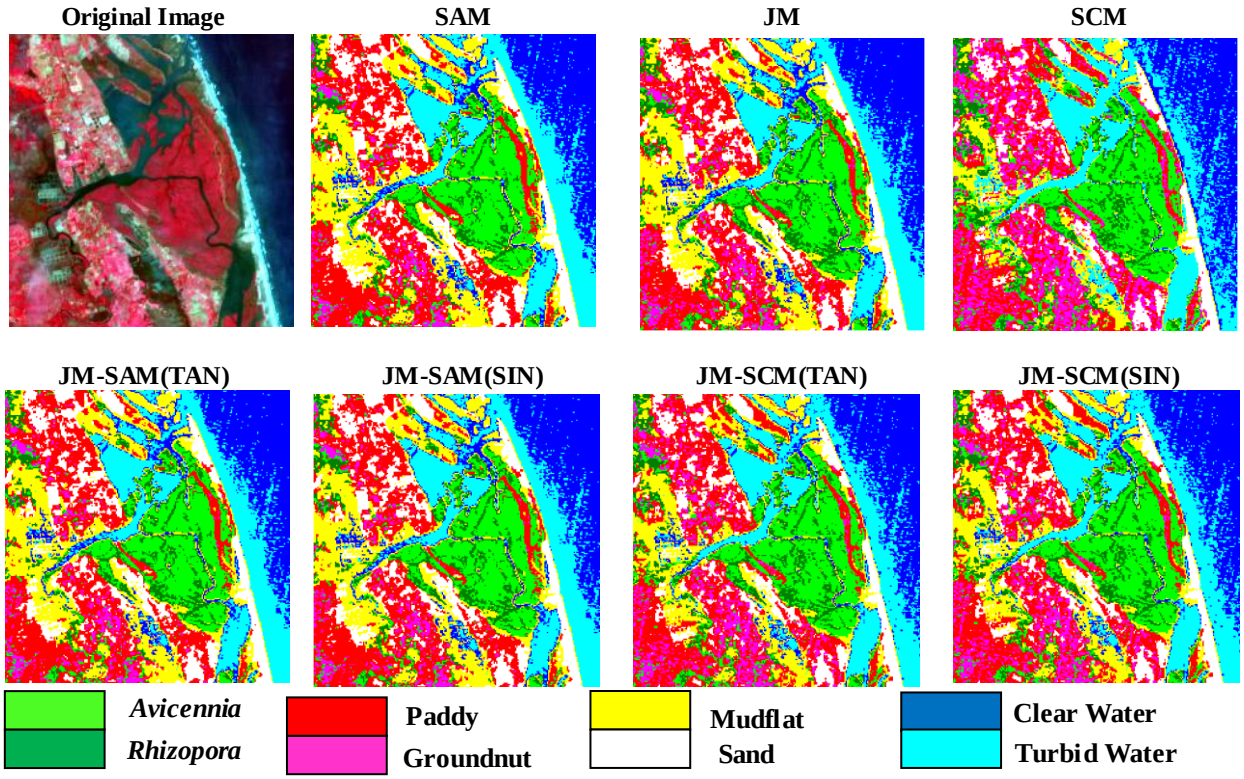

Figure1 Results of classification of Pichavaram region using EO-1 Hyperion image

3.2 Study Site II –Muthupet Mangrove Ecosystem, Southern India

The results of the classification based on the spectral matching approaches for SCM, JM-SCM(TAN), JM-SCM(SIN), SAM, JM, JM-SAM(TAN) and JM-SAM(SIN) are shown in Figure (4). The spectral matching values among the reference classes (*Avicennia*, *Prosopis*, plantation, marsh, mudflat, sand, clear water and turbid water follows the order: JM-SCM(TAN)<JM-SCM(SIN)<JM-SCM(TAN)<JM-SCM(SIN)<JM<SCM<SAM. The least matching values indicate a higher discrimination among the target and reference spectra.
The higher performance of the JM-SCM algorithms can be observed from the RSDPB plots as shown in the Figure 5. In the case of JM-SCM measures, RSDPB measures of the Avicennia class from the Prosopis and plantation classes was the (0.0047, 0.0124) and (0.0073, 0.0193) respectively. In the case of other measures ranging from JM-SAM(TAN), JM-SAM(SIN), JM, SCM and SAM, the RSDPB measures were (0.0145, 0.0195), (0.0236, 0.0552), (0.0549, 0.0635), (0.0134, 0.0184) and (0.0493, 0.0580) respectively. The least of JM-SCM measures in assessing the match for Avicennia among closely similar classes indicates its increased discriminability

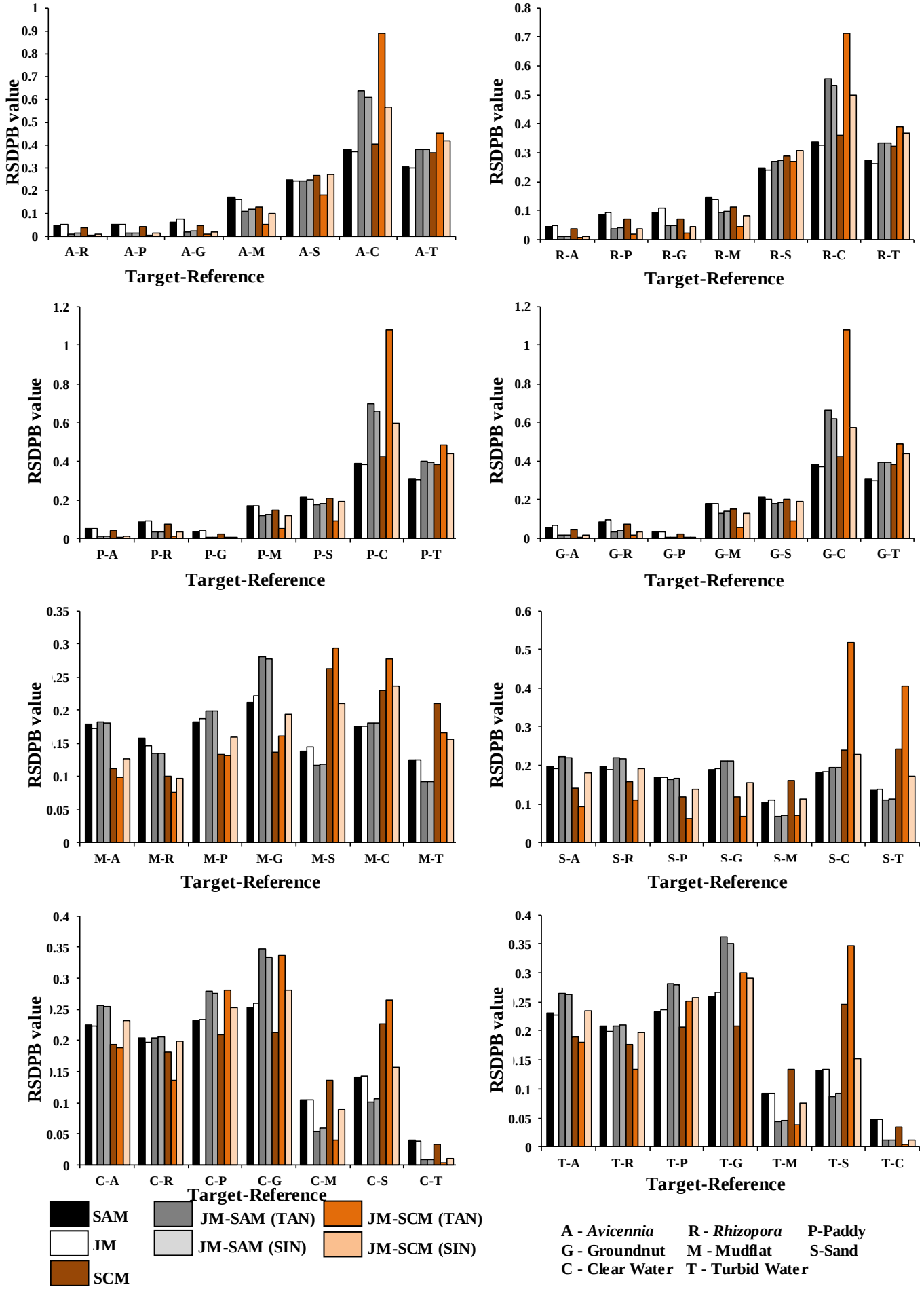

Figure 2 RSDPB plots for spectral matching measures applied to Pichavaram region using EO-1 Hyperion images

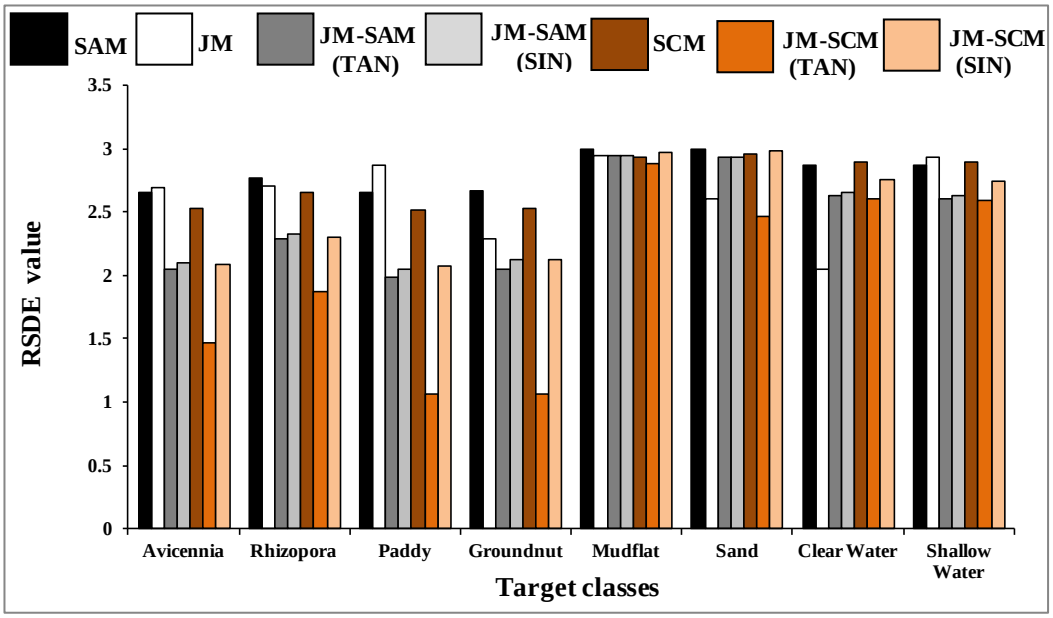

Figure 3 RSDE plots for spectral matching measures applied to Pichavaram region using EO-1 Hyperion images

Table 1 Variations of sensitivity and 100-specificity values for the matching measures for Pichavaram region

Matching Measures	*A*		*R*		P		G		M		S		C		T	
	Pd	Pf	Pd	Pf	Pd	Pf	Pd	Pf	Pd	Pf	Pd	Pf	Pd	Pf	Pd	Pf
	SMI		SMI		SMI		SMI		SMI		SMI		SMI		SMI	
SAM	70	30	100	30	40	20	75	70	75	40	64.3	10	100	20	100	10
	0.43		0.30		0.50		0.93		0.53		0.16		0.20		0.10	
JM	70	30	80	20	44.4	60	60	40	69.2	10	87.5	30	100	0	100	0
	0.43		0.25		1.35		0.67		0.14		0.34		0		0	
JM-SAM (TAN)	75	10	100	30	64.3	10	83.3	50	90.9	0	100	0	90.9	0	100	10
	0.13		0.30		0.16		0.60		0		0		0		0.10	
JM-SAM (SIN)	69.2	10	87.5	30	58.3	30	100	40	100	0	100	0	83.3	0	100	10
	0.14		0.34		0.51		0.40		0		0		0		0.10	
SCM	100	30	80	60	55.6	50	66.7	0	61.5	20	90.9	0	80	20	80	20
	0.30		0.75		0.90		0		0.33		0		0.25		0.25	
JM-SCM (TAN)	100	10	100	20	75	10	90.9	0	100	10	90.9	0	100	0	100	0
	0.10		0.20		0.13		0		0.10		0		0		0	
JM-SCM (SIN)	100	0	100	10	80	20	81.8	10	100	10	90.9	0	90	10	90	10
	0		0.10		0.25		0.12		0.10		0		0.11		0.11	

Note: *A-Avicennia, R-Rhizopora,* P-Paddy, G-Groundnut, M-Mudflat, S-Sand, C-Clear Water, T-Turbid Water
Pd- Probability of detection = Sensitivity , Pf-Probability of false alarm = 100-Specificty

This discrimination is reflected in the quantum of accuracy of classification where the JM-SCM(TAN) and JM-SCM(SIN) had an higher accuracy of 91.25 % and 88.75 %. The accuracy of JM-SAM(TAN), JM-SAM(SIN), JM, SCM, SAM were 85%, 83.75%, 76.25%, 75% and 70% respectively. The higher accuracy of JM-SCM measures is due to less uncertainty in identifying the correct matches which is shown as RSDE plots (Figure 6).
In the case of the sensitivity (Pd) and 100-specificity (Pf) values for *Prosopis* (Table 2), SCM has a lower detection rate of 66.7 % with a false alarm in the range of 40 %. From the accuracy assessment, it was observed that some of the target *Prosopis* are overestimated as *Avicennia* and plantation with a lower detection rate of 63.6% and 66.7%. This overestimation was suppressed as JM-SCM(TAN) and JM-SCM(SIN) resulted in a higher detection rate of (90.9%, 90.9%) and (83.3%, 70%) for *Avicennia* and plantation respectively. This was reflected in Table 2, where the SMI of JM-SCM measures in identifying *Prosopis* was the least (0.12, 0) compared to 0.60 of SCM. The SMI for JM-SCM measures in identifying each class was the least compared to other matching measures, thereby indicating its improved performance in yielding higher detection with lower false alarm.

4 CONCLUSIONS

This paper has presented a JM-SCM spectral matching approach which combines the capabilities of the Spectral Correlation Mapper (SCM) and the Jeffries-Matusita distance (JM) measure. The utility of the proposed algorithm in extracting information using hyperspectral images for a mangrove ecosystem has also been demonstrated. JM-SCM

approaches out-performed the individual measures of SCM and JM with an increased classification accuracy of (93.75 % and 91.25 %) and (91.25 % and 88.75 %) for the Pichavaram and Muthupet mangrove ecosystems. This is due to the property of JM and SCM to simultaneously utilize the spectral and spatial information of the entire length of the spectral vector. Further, it has been demonstrated that the correlation angle (SCM) is a superior parameter than spectral angle (SAM) since the JM-SCM measures outperformed JM-SAM measures. A significant outcome of this work is the introduction of a new parameter called SMI to quantify the strength of spectral match.

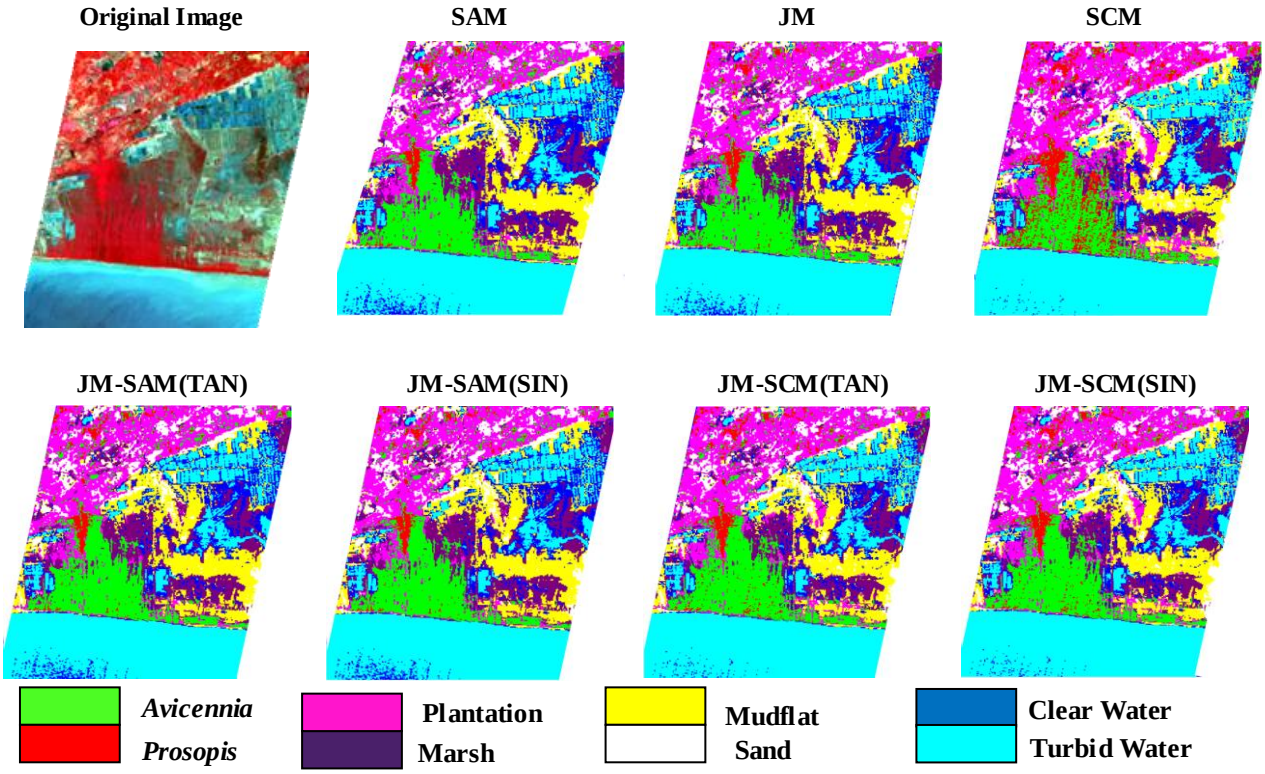

Figure 4 Results of classification of Muthupet region using EO-1 Hyperion image

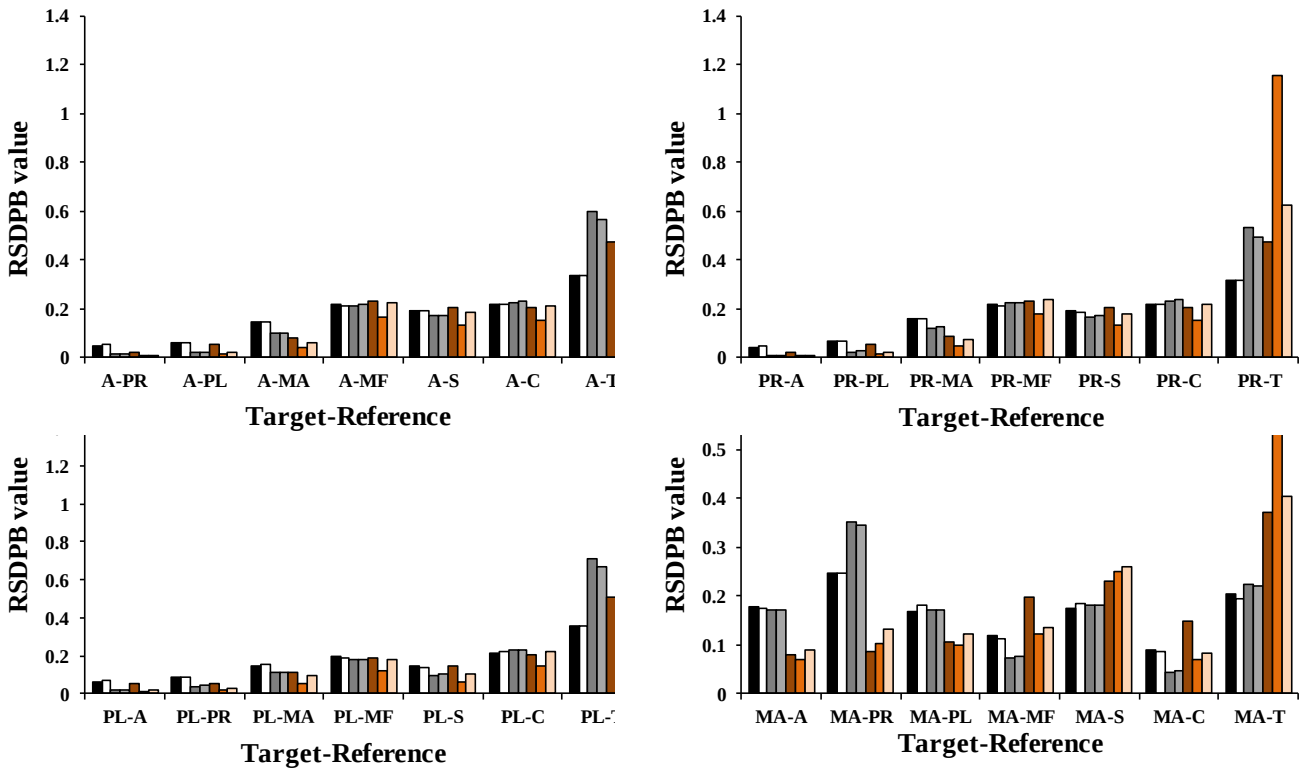

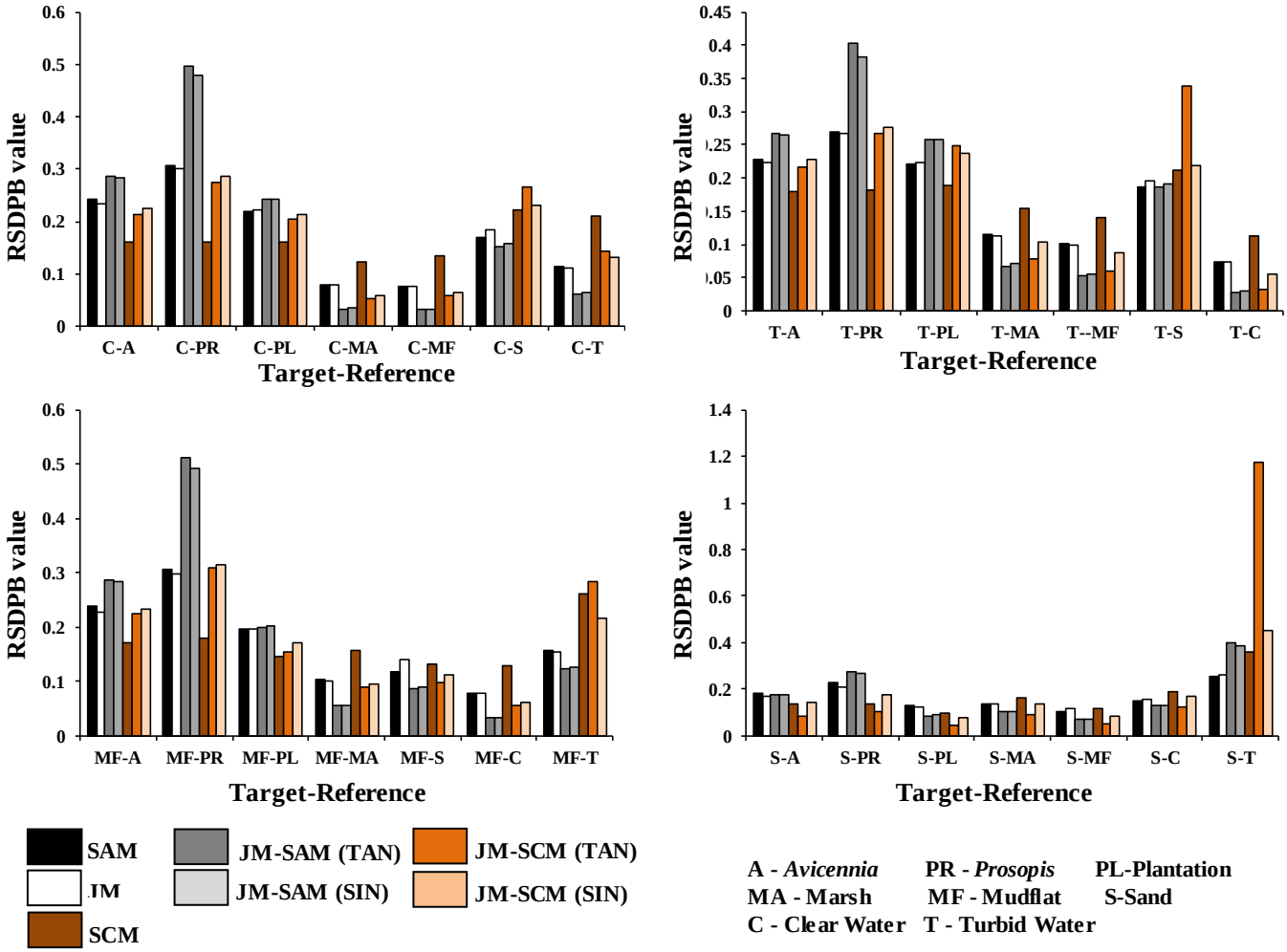

Figure 5 RSDPB plots for spectral matching measures applied to Muthupet region using EO-1 Hyperion images

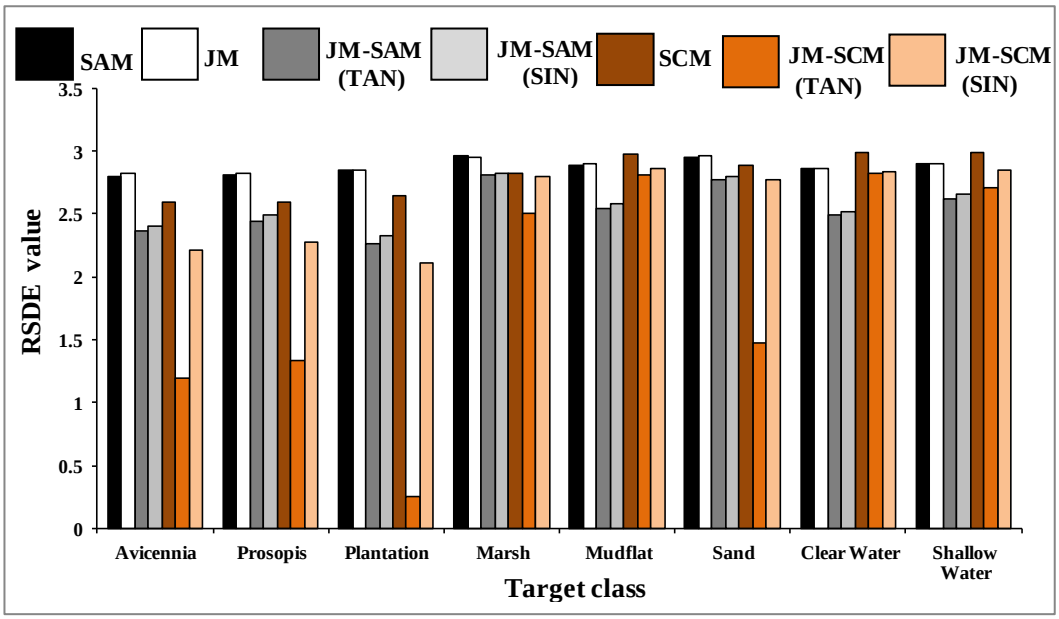

Figure 6 RSDE plots for spectral matching measures applied to Muthupet region using EO-1 Hyperion images

Table 2 Variations of sensitivity and 100-specificity values for the matching measures for Muthupet region

Matching Measures	*A*		*PR*		PL		MA		MF		S		C		T	
	Pd	Pf	Pd	Pf	Pd	Pf	Pd	Pf	Pd	Pf	Pd	Pf	Pd	Pf	Pd	Pf
	SMI		SMI		SMI		SMI		SMI		SMI		SMI		SMI	
SAM	100	30	36.4	60	36.4	60	75	10	83.3	50	71.4	0	81.8	10	100	20
	0.30		0.34		0.30		0.30		0.47		0		0		0	
JM	87.5	30	80	60	53.3	20	66.7	0	83.3	50	81.8	10	83.3	0	100	20
	1.65		0.75		0.28		0.30		0.60		0.20		0.30		1.65	
JM-SAM (TAN)	100	30	72.7	20	72.7	20	76.9	0	88.9	20	100	20	90.9	0	90	10
	1.65		0.38		0.28		0.33		0.30		0		0.43		1.65	
JM-SAM (SIN)	100	30	66.7	20	61.5	20	80	20	80.0	20	100	0	100	0	100	20
	0.13		0		0		0.25		0.39		0.30		0.11		0.60	
SCM	63.6	30	66.7	40	66.7	20	54.6	40	77.8	30	100	10	81.8	10	100	20
	0.60		0.60		0.23		0.25		0.39		0.30		0.11		0.60	
JM-SCM (TAN)	90.9	0	100	20	83.3	0	90	10	100	30	83.3	0	100	10	90.9	0
	0		0.12		0.20		0		0.10		0		0.11		0	
JM-SCM (SIN)	90.9	0	100	30	70	30	83.3	0	90	10	90.0	10	100	10	90.9	0
	0.12		0		0		0		0.12		0.10		0.10		0.12	

Note: *A-Avicennia*, *PR-Prosopis*, PL-Plantation, MA-Marsh, MF-Mudflat, S-Sand, C-Clear Water, T-Turbid Water
Pd- Probability of detection = Sensitivity , Pf-Probability of false alarm = 100-Specificty

REFERENCES

Alatorre, L. C., Sanchez-Andres, R., Cirujano, S., Begueria, S., & Sanchez-Carrillo, S. 2011. Identification of mangrove areas by remote sensing: The ROC curve technique applied to the northwestern Mexico coastal zone using Landsat imagery. Remote Sensing, *3*(8), pp.1568-1583.

Bertels, L., D. Bart, K. Pieter, D. Walter, and P. Sam. 2005. Optimized Spectral Angle Mapper Classification of Spatially Heterogeneous Dynamic Dune Vegetation, a Case Study Along the Belgian Coastline. In: 9th International Symposium on Physical Measurements and Signatures in Remote Sensing (ISPMSRS), Beijing, October 17–19.

Chang, C. I. 2000. An Information-Theoretic Approach to Spectral Variability, Similarity, and Discrimination for Hyperspectral Image Analysis. IEEE Transactions on Information Theory, 46(5), pp.1927–1932.

Chang, C. I., ed. 2003. Hyperspectral Imaging: Techniques for Spectral Detection and Classification. New York: Kluwer Academic.

De Carvalho, O.A. and Meneses, P.R. 2000. Spectral correlation mapper (SCM): an improvement on the spectral angle mapper (SAM). In: Summaries of the 9th JPL Airborne Earth Science Workshop, Vol. 9, JPL Publication.

Du, Y., C. I. Chang, H. Ren, C. C. Chang, J. O. Jensen, and F. M. D'Amico. 2004. New Hyperspectral Discrimination Measure for Spectral Characterization. Optical Engineering, 43(8), pp. 1777–1786.

Dudeni, N., and P. Debba. 2009. Evaluation of Discrimination Measures to Characterize Spectrally Similar Leaves of African Savannah Trees. In: 57th Biennial Session of the Int. Statistical Institute, South Africa, August16–22, 2009.

Granahan, J. C., and J. N. Sweet. 2001. An Evaluation of Atmospheric Correction Techniques Using the Spectral Similarity Scale. In: IEEE 2001 International Geoscience and Remote Sensing Symposium. Vol.5, pp.2022–2024.

Homayouni, S., and M. Roux. 2004. Hyperspectral Image Analysis for Material Mapping Using Spectral Matching. In: ISPRS Congress Proceedings, Istanbul, Turkey, July 12–23.

Kruse, F.A., Richardson, L.L. and Ambrosia, V.G. 1997. Techniques developed for geologic analysis of hyperspectral data applied to near-shore hyperspectral ocean data. In: Fourth International Conference on Remote Sensing for Marine and Coastal Environments, 17, pp. 19.

Li, H., W. S. Lee, K. Wang, R. Ehsani, and C. Yang. 2014. Extended Spectral Angle Mapping (ESAM) for Citrus Greening Disease Detection Using Airborne Hyperspectral Imaging. Precision Agriculture, 15(2), pp.162–183.

Naresh Kumar, M., V. R. Seshasai, K. S. Vara Prasad, V. Kamala, K. V. Ramana, R. S. Dwivedi, and P. S. Roy. 2011. A New Hybrid Spectral Similarity Measure for Discrimination among Vigna Species. International Journal of Remote Sensing, 32(14), pp. 4041–4053.

Padma, S., and S. Sanjeevi. 2014. Jeffries Matusita Based Mixed-Measure for Improved Spectral Matching in Hyperspectral Image Analysis. Int. Jour. of Applied Earth Observation and Geoinformation, 32(2014), pp.138–151.

Robila, S. A., and A. Gershman. 2005. Spectral Matching Accuracy in Processing Hyperspectral Data. IEEE International Symposium on Signals, Circuits and Systems, 1, pp.163–166.

Shanmugam, S., and SrinivasaPerumal, P. 2014. Spectral matching approaches in hyperspectral image processing. International Journal of Remote Sensing, 35(24), pp. 8217-8251.

Staenz, K., J. Schwarz, L. Vernaccini, F. Vachon, and C. Nadeau. 1999. Classification of Hyperspectral Agricultural Data with Spectral Matching Techniques. In: Int. Symposium on Spectral Sensing Research (ISSSR 99), Las Vegas.

Vishnu, S., R. R. Nidamanuri, and R. Bremananth. 2013. Spectral Material Mapping Using Hyperspectral Imagery: A Review of Spectral Matching and Library Search Methods. Geocarto International 28(2), pp. 171–190.